Asynchronous Hyperbolic UWB Source-Localization and Self-Localization for Indoor Tracking and Navigation

Chiasson, David; Lin, Yuan; Kok, Manon; Shull, Peter

DOI
10.1109/JIOT.2023.3243384

Publication date
2023

Document Version
Final published version

Published in
IEEE Internet of Things Journal

Asynchronous Hyperbolic UWB Source-Localization and Self-Localization for Indoor Tracking and Navigation

David Chiasson, Yuan Lin, *Graduate Student Member, IEEE*, Manon Kok, and Peter B. Shull, *Member, IEEE*

***Abstract*—Hyperbolic localization measures the time difference of arrivals (TDOAs) of signals to determine the location of a wireless source or receiver. Traditional methods depend on precise clock synchronization between nodes so that time measurements from independent devices can be meaningfully compared. Imperfect synchronization is often the dominant source of error. We propose two new message-based TDOA equations for hyperbolic localization which require no synchronization and meet or exceed state-of-the-art accuracy. Our approaches leverage anchor nodes that observe each other's packet arrival times and a novel reformulation of the TDOA equation to reduce the effect of clock drift error. Closed-form equations are derived for computing TDOA in both self-localization and source-localization modes of operation along with bounds on maximum clock drift error. Three experiments are performed, including a clock drift simulation, a nonline-of-sight (NLOS) simulation, and an indoor validation experiment on custom ultra wideband (UWB) hardware all of which involved eight anchor nodes and one localizing node in a 128-m^3 capture volume. Our source-localization approach achieved unprecedented accuracy with lower cost equipment and trivial setup. Our self-localization matched state-of-the-art accuracy but with infinite scalability and high privacy. These results could enable economical and infinite density indoor navigation and dramatically reduce the economic cost and increase the accuracy of implementing industrial and commercial tracking applications.**

***Index Terms*—Hyperbolic localization, indoor navigation, multilateration, time difference of arrivals (TDOA), ultra wideband (UWB).**

I. Introduction

RADIO localization utilizes knowledge about wave propagation to determine the location of a radio source or receiver. Localization is a valuable service across countless industrial, commercial, public, and military applications. As such, many mature systems have been developed to provide these services, including Loran-C [1], GPS [2], BeiDou [3], Galileo [4], cellular network localization [5], and many more. One of the frontiers in localization technology is that of indoor localization [6]. Indoor localization is difficult because it requires relatively high levels of precision, and physical structures can occlude weak signals such as those from global navigation satellite systems (GNSS). Additionally, indoor localization systems will generally cover a smaller area than other localization systems, placing a heavier burden on low-cost and simple infrastructure before it is economically feasible to implement since costs cannot be shared.

Ultra wideband (UWB) has emerged as a promising technology for indoor localization [7]. The high temporal resolution of the UWB impulses allow precise measurement of signal transmission and reception relative to narrow-band alternatives. This is because additive noise or interference is less likely to affect detection time. From this information, time-of-flight (TOF) and, thus, range between two transceivers can be deduced. Using this timing information to achieve localization has thus far proven more accurate than relying on other features of the wireless channel, such as the direction of propagation, or signal attenuation [6], [8]. UWB localization has been shown to achieve decimeter or centimeter-level accuracy under ideal conditions [9] and even better when combined with IMU [10]. In comparison to narrow-band alternatives, UWB systems can safely omit the base-band conversion stage which somewhat simplifies the signal processing. However, supporting larger bandwidths and higher frequencies may increase demands on RF filters, amplifiers, ADC, and antennas. UWB has also been shown to be useful for security and data transfer applications [11], [12].

These advantages of UWB have caused it to achieve wide acceptance in recent years. UWB is a popular choice for factory asset tracking [13] and other industrial logistic applications. Recent releases of consumer electronics have also embraced UWB. Apple, Samsung, and Xiaomi have all announced UWB capable devices [14] and Google has released an UWB Android API. Several automobile makers have incorporated UWB in their products [15].

However, several problems still exist that prevent UWB from being utilized for some indoor localization applications [8]. First, the accuracy achieved by many real-word implementations of UWB localization are far from ideal. Factors, such as nonline-of-sight (NLOS) and calibration sensitivity greatly degrade performance [16]. Additionally,

Manuscript received 12 November 2022; revised 18 January 2023; accepted 3 February 2023. Date of publication 15 February 2023; date of current version 23 June 2023. This work was supported in part by the National Natural Science Foundation of China under Grant 51875347. *(Corresponding author: David Chiasson.)*

David Chiasson, Yuan Lin, and Peter B. Shull are with the State Key Laboratory of Mechanical System and Vibration, School of Mechanical Engineering, Shanghai Jiao Tong University, Shanghai 200240, China (e-mail: dchiasso@sjtu.edu.cn; pshull@sjtu.edu.cn).

Manon Kok is with the Delft Center for Systems and Control, Delft University of Technology, 2628 CD Delft, The Netherlands.

Digital Object Identifier 10.1109/JIOT.2023.3243384

	Method	Accuracy	Power	Scalability	Infrastructure	Privacy	Complexity/Cost Anchor	Complexity/Cost Tag
Tracking Applications	*Traditional* TDOA	med	low	high	high	low	high	low
	Proposed Hyperbolic source-localization	high	low	high	low	low	med	low
Navigation Applications	*Traditional* AltDS-TWR	high	high	low	low	low	med	med
	Proposed Hyperbolic self-localization	high	med	∞	low	high	med	med

Fig. 1. Qualitative comparison of the two proposed methods (hyperbolic source-localization and hyperbolic self-localization) with the two most common alternatives (Traditional TDOA and AltDS-TWR). Higher is better for accuracy, scalability, and privacy while lower is better for power, infrastructure and complexity. The most significant improvements provided by the proposed methods are highlighted in gray.

traditional time difference-of-arrival (TDOA) methods is often used in practice instead of more accurate TOF methods [17] due to application requirements, such as node density and power consumption. The localization accuracy of traditional TDOA methods are limited by clock drift while modern Double-Sided Two-Way TOF methods are not [18]. This causes some applications to suffer from meter-level error instead of the centimeter-level error of ideal conditions. Second, infrastructure requirements are too costly and difficult to deploy [5]. Even though UWB transceivers are conceptually simpler than narrow band, the TDOA method generally preferred in industrial applications depends on precise clock synchronization between anchor nodes. This leads to expensive and bulky clock hardware, complex synchronization algorithms, and high system sensitivity to any anchor disturbances. These costs can be tolerated in some industrial applications if the economic incentive is compelling, but it provides a discouragement for many consumer applications. Finally, there is the issue of privacy. A highly accurate indoor localization system would reveal information which consumers may feel uncomfortable revealing to service providers or others. This dynamic has been an accuracy limiting factor in the related application of cellular localization [5].

This study proposes two new TDOA equations for UWB localization which improve or solve all of these problems. We propose one method to address tracking applications which we refer to as source-localization in which a network of known location anchors determines the location of the localizing node. We propose a second method to address navigation applications which we refer to as self-localization in which a network of anchors provide a service which allows the localizing node to resolve its own location. Our source-localization method has higher accuracy and lower infrastructure requirements than existing methods. Our self-localization method provides high privacy and infinite localizing node density as the localizing nodes do not perform any transmissions. Both methods achieve the highest previously demonstrated UWB localization accuracy but using new approaches which provide many valuable application benefits, such as scalability, hardware simplicity, power conservation, ease of deployment, and privacy (Fig. 1).

The high level of localization accuracy is achieved by minimizing the effects of clock drift which contribute to synchronization error. According to [19], "In UWB TDOA localization systems, anchor synchronization errors are the main performance limiting factors." This synchronization error leads to an inability to accurately measure time and compare between independent devices. According to a localization survey by Li et al. [20], "Minimizing error in time of arrival and other time-based measurements is the greatest challenge in many source localization studies." Our proposed methods can eliminate synchronization error due to clock drift as a significant source of error in many applications.

While existing UWB localization methods based on TOF can effectively eliminate clock drift error, these methods have several disadvantages, namely, scalability, power consumption, and privacy [8], [17]. To provide these additional benefits, we instead take a TDOA approach to UWB localization. Our methods differ from previous TDOA approaches in that anchors record ranging messages from other anchors in addition to those from the localizing nodes. We then use a formulation of the TDOA equation which is strategically chosen to reduce error due to clock drift. Our methods do not require any synchronization between anchor nodes which significantly decreases system complexity and cost compared with other TDOA approaches.

II. Background

Localization applications generally attempt to find the location of some object(s) in the context of a fixed reference frame. Radio localization usually utilizes several nodes, known as anchors, which are at known locations in the reference frame. The localizing node is at an unknown location and depending on the application can be called mobile node, tag, client, or user. While localization system can be designed to locate passive objects (i.e., radar systems) the present work will focus on active objects that can either transmit or receive radio messages to assist in the localization process.

Radio localization methods utilize some known characteristic of wave physics and the interaction with the wireless channel in order to deduce location. Commonly utilized

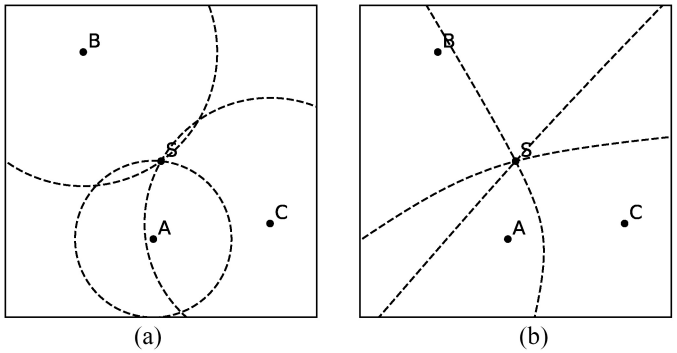

Fig. 2. Two common time-based radio localization approaches. A, B, and C are anchor nodes while S is the localizing node. Each approach can be applied to tracking applications (source-localization) or navigation applications (self-localization). (a) TOF. (b) TDOA.

characteristics include attenuation rate, propagation direction, and propagation speed. These characteristics can and are used in conjunction with each other to develop hybrid systems [21]. This work will focus on timing-based methods for radio localization, but alternatives include receive signal strength [22], [23], angle of arrival [24], [25], and fingerprinting [26], [27].

A. Time of Flight

TOF is a timing-based metric which depends on a known propagation speed for the wireless signal, i.e., the speed of light. TOF methods attempt to measure the time difference between signal transmission and reception and then multiply by propagation speed to achieve range. This produces a sphere of possible locations for the localizing node with the anchor at the center. The information from several anchors must be combined to perform true-range multilateration as demonstrated in Fig. 2(a). These methods are sometimes referred to as ranging. Two methods for asynchronous TOF-based ranging are included in IEEE standard 802.15.4a [28]. The first of these is two-way ranging (TWR). This method uses a request and response message. The initiator and responder both measure the time period between these two messages, the difference of which is twice the TOF. This method eliminates clock offset, but does not account for clock drift. This clock drift error is significant. If clocks are used which adhere to IEEE 802.15.4a accuracy standards (20 ppm) [28], and the response delay was 1ms, the TWR method would experience around 10m of error due to clock drift. This weakness was the motivation for the second method, symmetric double-sided TWR (SDS-TWR). SDS-TWR adds an additional message to the TWR process and then computes TOF in a way that essentially eliminates error due to clock drift. This is possible since the TWR process is repeated in the other direction, producing an inverse error which can then cancel out the error from the first TWR. However, in order to achieve this accuracy, the period of time between the request–response messages and response-final messages must be identical, i.e., symmetric. This requirement limits the scalability of the ranging system [29]. While several TOF-based ranging methods have been proposed since the publication of the IEEE standards, the most convenient is alternative double-sided TWR (AltDS-TWR) [29]. This method uses the same message passing pattern as SDS-TWR, but proposes an alternative equation for computing TOF. The AltDS-TWR equation is mathematically equivalent to that used in SDS-TWR in the absence of clock drift. However, in the presence of clock drift, the AltDS-TWR method is nearly unaffected in indoor localization applications while SDS-TWR can become unusable if response times are asymmetric.

Due to the high accuracy of these TOF methods, they are commonly used in UWB research studies. However, they still have certain disadvantages compared with TDOA methods. The bidirectional communication puts significant demands on the power consumption and complexity of the localizing nodes. Many localization systems find it economical to push as much complexity away from the localizing node and onto the anchor network as possible. These methods can also have scaling issues due to the large number of messages required.

B. Time Difference of Arrival

TDOA, also known as hyperbolic localization, is a timing-based metric which depends on a known propagation speed for the wireless signal. However, instead of directly measuring TOF between a node and each anchor, TDOA methods measure the difference in TOF between two links. If the difference in transmission time is known, this can be deduced from the difference in time of arrival. UWB TDOA has long been used for localization applications [30], [31], [32], [33], [34], [35]. In practice, these systems will sometimes formulate their signal processing in terms of pseudo-ranges which is the real range plus an unknown clock offset. An equivalent TDOA formulation can be achieved by taking pairs of pseudo-range equations and subtracting them. If TDOA is observed between two known-location anchors to the localizing node, we can compute a hyperboloid of possible locations for the localizing node with anchors at the two foci [Fig. 2(b)]. Repeating this process with several pairs of anchors allows us to perform pseudo-range multilateration and resolve the position of the localizing node. TDOA-based methods have also been referred to as hyperbolic positioning or just multilateration. In this context, hyperbolic source-localization and self-localization have been referred to as forward and reverse TDOA, respectively, [36].

A large portion of existing localization systems utilize TDOA methods. One reason for this is that TDOA methods do not necessarily need to know the moment of signal transmission for source-localization or the absolute moment of signal reception for self-localization. Applications have historically taken advantage of this feature by designing highly asymmetric system complexity such that anchor nodes will be orders of magnitude more complex and expensive than the localizing node. This has significant economic benefits if there are many more localizing nodes than there are anchors. As such, industrial asset tracking with UWB is generally done using TDOA-based hyperbolic source-localization [37]. Loran-C was the first widespread radio localization system used throughout North America and Europe and it uses a form

of hyperbolic self-localization [1]. GNSS also provide hyperbolic self-localization services. However, most GNSS systems differ from the TDOA methods proposed in this work in that they are not message-based. Usually, the anchors [known as satellites or Space Vehicles (SV)] broadcast a continuous signal that the localizing node can lock onto. This essentially provides a way for localizing nodes to borrow the high quality clocks of the anchor nodes albeit with a fixed time offset. GNSS processing therefore must account for clock offset but not clock drift.

C. Hyperbolic Localization Related Work

In this section we discuss the current state-of-the-art in hyperbolic localization with an emphasis on studies most related to this work. This discussion is divided into two sections, tracking applications which utilize source-localization methods and navigation applications which utilize self-localization methods.

1) Tracking Applications: Tracking applications, or source-localization are the most commonly implemented form of TDOA localization. Such implementations usually contain a wired backbone to synchronize anchor nodes [38]. Wireless methods have also been developed although they generally are less accurate than wired methods [39], [40]. Using either approach, clock accuracy remains a difficult problem often causing increase in localization error, system complexity and hardware cost [20]. As such, many works have explored other methods for reducing this error source in hyperbolic localization approaches. Several proposed methods utilize a filtering or modeling approach to address this problem [18], [34]. These approaches model the clock drift of anchors and account for them during processing. These methods will introduce a filter delay, sacrifice some high-frequency information, as well as sometimes requiring coordinated transmissions times.

He and Dong [40] proposed asynchronous TDOA (A-TDOA) which requires the localizing node to perform immediate retransmissions of anchor beacons. Although called TDOA, this method relies on the intersection of ellipsoids instead of hyperboloids. While their method does eliminate the need for node synchronization, it pays a high price for it in terms of power, privacy, accuracy, and scalability. For practical applications, it struggles to provide advantages over AltDS-TWR.

Xue et al. [39] proposed Async-TDOA which utilizes an additional anchor node to transmit a reference signal which is used to adjust for clock drifts using an interpolation method. This method requires an additional anchor node, and does not have a known error limit. Zhou et al. [41] proposed difference-TDOA (D-TDOA) which utilizes a similar message passing pattern as our proposed hyperbolic source localization method. However, their approach does not solve clock drift in general, only in the special case where the round trip transmission (RTT) has a 1:2 ratio. This has similar problems as those experienced by SDS-TWR [29], namely, that ranging messages cannot be reused in multiple simultaneous ranging processes, thus limiting the scalability of the system.

2) Navigation Applications: Navigation applications have been less explored in the literature and is a more difficult problem. Tracking applications using TDOA can achieve anchor synchronization by using a wired backbone, and the clock drift of the localizing node can be ignored. Navigation applications on the other hand generally cannot ignore clock drift on the localizing node. The mobile nature of the localizing node also precludes a wired synchronization approach.

Attempts have been made to perform wireless synchronization through measuring and correcting for relative clock skews [42]. Such approaches are useful, although they are still significantly lower accuracy than the best TOF-based approaches which suggests that imperfect synchronization is still a dominant source of error.

Großwindhager et al. [43] proposed SnapLoc, a system design in which the anchors transmit at nearly the same moment. The localizing node then analyzes the channel impulse response (CIR) to deduce TDOA estimates. Since the time between anchor messages is so small in this method, the drift of the localizing node's clock is negligible. However, getting the anchors to transmit with such precision is a difficult problem, encouraging the usage of wire synchronized anchors which still struggle to match the accuracy of TOA methods.

III. Methods

In this section, we derive the equations we use to compute TDOA (T_Δ) in source-localization and self-localization configurations. We assume a scenario with one localizing node at an unknown location and a network of anchor nodes at known locations. All nodes are independent and unsychronized, thus suffering from relative clock offset and drift. The goal of these derivations is to find a formula for computing TDOA (T_Δ) which can cancel out the effects of clock offset and clock drift. An overview of our two proposed methods in comparison to AltDS-TWR and Round Robin Ranging can be found in Fig. 3. Two methods are presented and theoretical limits on error due to clock drift are derived. Finally, a simulation experiment and a validation experiment are presented which we use to confirm our theoretical results.

The error model we use in our derivations is as follows. Each anchor and the mobile node has an independent clock with a time offset (c) and clock drift (e) due to hardware imperfections, temperature variance, different starting times and other factors. Thus, each node has an imperfect measurement of real time which we model as

$$\hat{t} = (1 + e)t + c = kt + c. \tag{1}$$

This model need only be accurate over the period of our ranging process which requires milliseconds to complete. Our model assumes a constant drift which may be reasonable since changes in drift will likely be affected by factors, such as temperature, which change on the scale of minutes. In line with the IEEE 802.15.4a standard [28], we consider clocks of quality ± 20 ppm which means $e = \pm 2 * 10^{-5}$.

Note that due to the symmetry of the wireless channel, TOFs between nodes are implicitly assumed to be symmetric in all our derivations (i.e., $T_{ab} = T_{ba}$). This may not strictly be true

if nodes are moving at high speeds. The error contribution of movement has been explored in [44] and is beyond the scope of this work.

Both proposed methods considered in this work are based on nodes measuring periods of time instead of moments in time. This serves to eliminate all clock offset factors since $\hat{T} = \hat{t}_1 - \hat{t}_0 = (1 + e)T = kT$. The methods proposed in this section will thus seek to reduce the error due to clock drift, e, while providing valuable application benefits, such as scalability, hardware simplicity, power conservation, ease of deployment, and privacy.

Both our proposed hyperbolic localization methods solve for TDOA $T_\Delta := T_{bs} - T_{as}$ which provides a hyperboloid of possible locations. This section demonstrates the calculation and error bounds of T_Δ for one localizing node and two anchor nodes. This process must be repeated with more anchor nodes until four or more hyperboloids have been determined for 3-D localization. The intersection of these hyperboloids can then be used as the location estimate. In practice, this is often done through linearizing the hyperbolic equations via Taylor-series expansion and iteratively performing linear regression as the hyperbolas will not precisely intersect [45]. Error bounds derived in this section are computed for T_Δ instead of for location since the final location error is dependent on many application specific factors, such as the number of anchors and geometric dilution of precision (GDOP).

A. Source-Localization

Hyperbolic source-localization, also known as forward TDOA, is designed for tracking applications. Fig. 3(c) demonstrates the proposed ranging process to measure TDOA for two anchors and one mobile node in a source-localization application. The anchor nodes A and B transmit messages and listen for messages from the mobile node S or for messages from other anchors. The mobile node only needs to transmit a message containing its unique identifier and can remain in a low-power sleep mode for the vast majority of the time. It is possible for a system to localize without the mobile node performing any listening and with the localization beacon occurring at an arbitrary point in time. However, some system designs require some information transfer to the mobile node in order to perform TDMA scheduling as is useful to avoid collisions in the presence of high mobile node density or high update rates [33]. The time periods measured by the anchor messages must be communicated to each other or some central processor in order to compute T_Δ. If the anchors are disconnected from any infrastructure, this could be done as the payload of their beacon signals. For example, node A could transmit a measurement of time periods D_{a1} and D_{a2} to node B as part of its final transmission. This would provide node B with enough information to compute T_Δ.

This ranging process demonstrated in Fig. 3(c) produces a single hyperboloid of possible locations and, thus, must be repeated with additional anchors to resolve the 3-D location of a mobile node. Note that each message can be simultaneously used in many TDOA estimation equations. For example, the mobile node S need only perform a single transmission regardless of the number of anchors present.

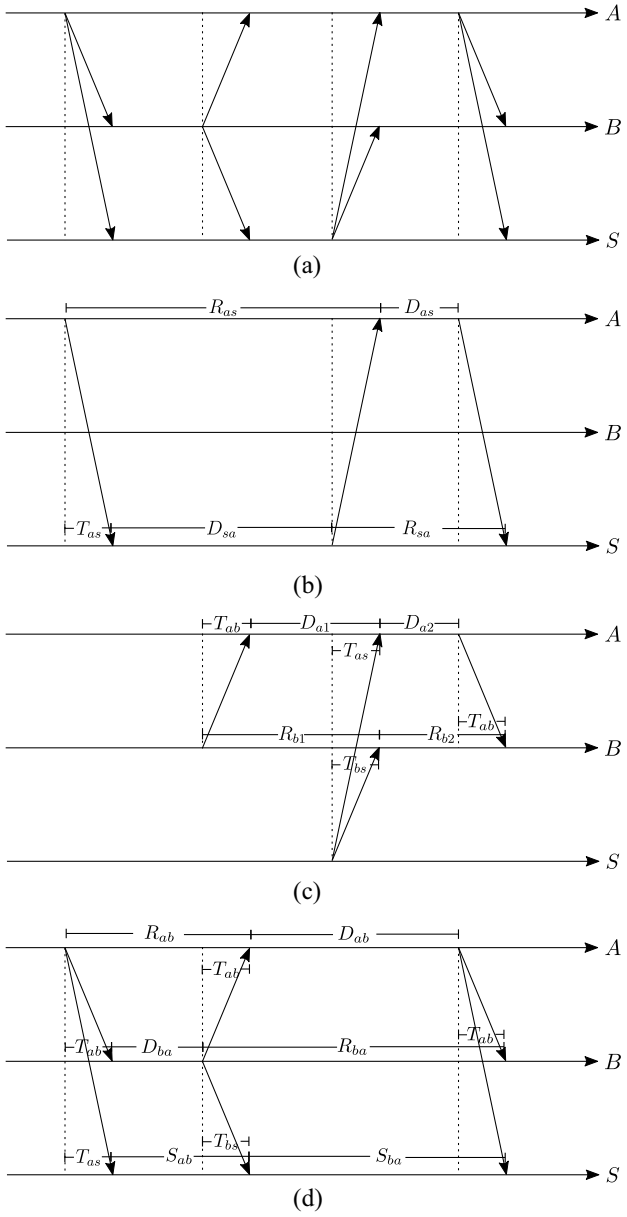

Fig. 3. Message passing and timing measurements required for proposed localization methods and reference method. A and B are anchor nodes while S is the localizing node. Each horizontal line is the timeline for that node while the transverse lines are wireless beacons. Each node is limited to observing with an imperfect clock the moments at which it sends or receives a beacon. Thus, T_{xx} cannot be observed directly and must be computed from D_{xx}, R_{xx}, and/or S_{xx} measurements. These figures are not to scale. In actuality, the TOF values (T_{ij}) are many orders of magnitude smaller than the time between messages. This message passing repeats with the last transmission of one cycle being the first transmission of the next cycle. (a) *Round Robing Ranging:* Ranging process used in our validation experiment. This method is a superset of all other methods. (b) *AltDS-TWR:* Previous high accuracy UWB localization method. Used as a comparison for the accuracy of our proposed methods. (c) *Hyperbolic Source-Localization:* Proposed method for tracking applications. (d) *Hyperbolic Self-Localization:* Proposed method of navigation applications.

The message timing required for this method [Fig. 3(c)] can be implemented by having each anchor transmit at a fixed interval. Collisions could be avoided by having one anchor

serve as a reference to provide a common time period at the expense of creating a single point of failure. The timing and order of anchor transmissions is not important, and a new localization estimation can be computed any time all anchors have transmitted once and the localizing node has transmitted once. If anchor transmissions are happening on a periodic basis, then a location estimate can be made with every transmission, as all TDOAs involving the transmitting node (anchor or localizing node) could be computed, although this may lead to error correlation between consecutive estimates.

1) Derivation: We now derive the proposed equation for $T_\Delta := T_{bs} - T_{as}$ using the information provided by the ranging process in Fig. 3(c). Following loops on the graph produce the following two equations:

$$\begin{aligned} R_{b1} &= T_{ab} + D_{a1} + T_{bs} - T_{as} \\ &= T_{ab} + D_{a1} + T_\Delta \end{aligned} \tag{2}$$

$$\begin{aligned} D_{a2} &= R_{b2} - T_{ab} + T_{bs} - T_{as} \\ &= R_{b2} - T_{ab} + T_\Delta. \end{aligned} \tag{3}$$

We multiply these together to get

$$\begin{aligned} R_{b1}D_{a2} = T_{ab}R_{b2} - T_{ab}^2 + D_{a1}R_{b2} - T_{ab}D_{a1} \\ + T_\Delta(R_{b2} + D_{a1} + T_\Delta). \end{aligned} \tag{4}$$

By using (2) to eliminate the T_Δ within the parenthesis and solving for the remaining T_Δ, we arrive at our TDOA equation for source-localization

$$T_\Delta = \frac{R_{b1}D_{a2} - D_{a1}R_{b2} - T_{ab}R_{b2} + T_{ab}D_{a1} + T_{ab}^2}{R_{b2} + R_{b1} - T_{ab}}. \tag{5}$$

All R and D values can be measured directly by their respective nodes although they experience several sources of error with clock drift dominating. T_{ab} is usually fixed since the anchor nodes are stationary and in known locations. However, if either of these are not the case, existing TWR techniques such as AltDS-TWR [29] can be applied between the anchors to compute T_{ab} in real time without requiring any additional transmissions.

2) Error Bounds: According to our error model of independent, low-cost clocks on anchor and mobile nodes, our observation of the time periods in (5) will be inexact. In this section, we derive bounds on the error contribution of clock error and drift. Note that the error bounds computed here are from a single source and will not reflect the total localization error experienced in practice.

A time period R measured directly by node i will be distorted according to that node's clock drift $\hat{R}_i = k_i R = (1+e_i)R$. This also applies to D and S measurements. The TOF between anchor nodes, T_{ab} is not measured directly by any one node. However, the information provided by our ranging method is enough to compute these values using AltDS-TWR [29]. In [29], several methods are presented for computing the TOF between two nodes i and j such that the observed distortion due to clock drift can be either $\hat{T}_{ij} = k_i T_{ij}$ or $\hat{T}_{ij} = k_j T_{ij}$. We can therefore consider the error experienced by our T_{ab} estimate to be either $e_a T_{ab}$ or $e_b T_{ab}$ depending on convenience. These error values are used in our derivations, although smaller errors could be achieved if anchor locations are stationary and known. The information required to compute T_{ab} is present if the source-localization ranging process shown in Fig. 3(c) is repeated. Using the above error models, we can compute bounds for error due to clock drift a

$$\begin{aligned} \text{error} &= \hat{T}_\Delta - T_\Delta \\ &= \frac{k_a k_b\left(R_{b1}D_{a2} - D_{a1}R_{b2} - T_{ab}R_{b2} + T_{ab}D_{a1} + T_{ab}^2\right)}{k_b(R_{b2} + R_{b1} - T_{ab})} - T_\Delta \\ \text{error} &= (k_a - 1)T_\Delta \\ \text{error} &= e_a T_\Delta. \end{aligned} \tag{6}$$

This is the source-localization method's TDOA error in seconds. To convert to meters we multiply both sides by the speed of light and the error is e_a times the range difference between the mobile node to anchor B and the mobile node to anchor A. Since e_a is very small ($\pm 2 * 10^{-5}$ according to the IEEE 802.15.4a standard [28]) this error will be very small for short and medium-range applications (applications with distances less than 10^5m).

Alternatively, we could have substituted (3) into (4) instead of (2) to achieve this equivalent formulation

$$T_\Delta = \frac{R_{b1}D_{a2} - D_{a1}R_{b2} - T_{ab}R_{b2} + T_{ab}D_{a1} + T_{ab}^2}{D_{a1} + D_{a2} + T_{ab}}. \tag{7}$$

Which would then experience error

$$\text{error} = e_b T_\Delta. \tag{8}$$

Both of these error bounds depend on the drift of only one anchor clock. This provides the opportunity to pick the anchor with the highest quality clock as a basis for computation which can further increase accuracy.

3) Comparison to Existing Methods: The proposed source-localization method is most closely comparable to traditional forward TDOA shown in Fig. 4(a). In traditional forward TDOA, the localizing node broadcasts a message to the anchor network and each anchor records the time of reception. Pairs of anchors, with knowledge of their locations, can determine a hyperboloid of possible locations for the localizing node by subtracting their measurements

$$T_\Delta = T_b - T_a. \tag{9}$$

This process can then be repeated with other anchors to resolve the 3-D location of the localizing node. This method is highly sensitive to the synchronization of the anchor node clocks. This synchronization method must proceed in parallel with to the location beacons shown in Fig. 4(a). If a synchronization method eliminates clock offset between nodes, clock drift will quickly degrade the accuracy leading to worst case

$$\text{error} = (e_a + e_b)T_{\text{sync}} \tag{10}$$

where T_{sync} is the period in seconds for one iteration of the synchronization process. This would produce meters of error if the synchronization method operated at 1000 Hz. Because of this, traditional forward TDOA must accurately estimate both the clock offset and drift components of (1) for each anchor node in addition to performing synchronization often. While a wired backbone is often used to perform synchronization in practice [38], several wireless methods have been implemented

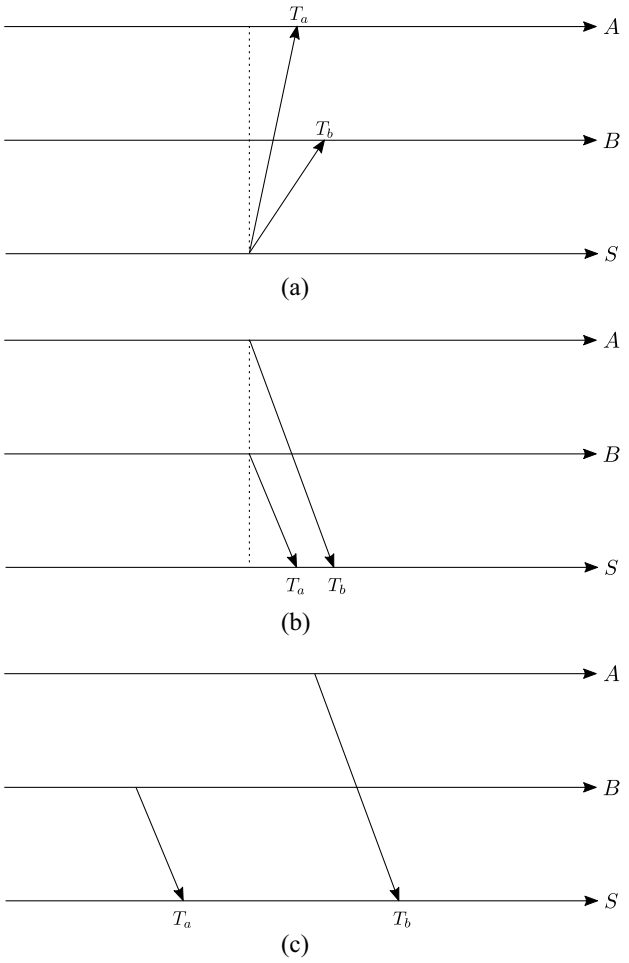

Fig. 4. Message passing for traditional TDOA localization methods with three nodes. A and B are anchor nodes while S is the localizing node. Each horizontal line is the timeline for that node while the transverse lines are wireless beacons. These methods require strict synchronization between the clocks of each node otherwise T_a and T_b cannot be meaningfully compared. (a) Traditional forward TDOA for source-localization or source applications. (b) Synchronous or concurrent reverse TDOA for self-localization or navigation applications. (c) Asynchronous reverse TDOA for self-localization or navigation applications.

in [33], [39], and [40] although they may suffer from slight accuracy degradation compared with wired solutions.

The proposed source-localization method sidesteps this complexity by integrating the ranging and synchronization processes. As will be shown below, clock offset and drift are implicitly accounted for in the proposed TDOA estimation equation leading to low clock drift error which is not dependant on the sampling period.

B. Self-Localization

Self-localization, also called reverse TDOA, is intended for navigation applications where the mobile node needs to ascertain their own location. Fig. 3(d) demonstrates the proposed ranging process to measure TDOA for two anchors (A and B) and one mobile node (S) in a self-localization application. The anchor nodes A and B transmit messages and listen for messages from other anchors. The mobile node S receives the anchor node transmissions but does not need to make any transmissions itself. The messages from the anchor nodes must contain a unique identifier, their location, and the time period measurements shown in Fig. 3(d) as measured by their local clock. Node A would transmit a measurement of time periods R_{ab} and D_{ab} while node B would transmit a measurement of time periods R_{ba} and D_{ba}. With enough anchors, this will provide the mobile node with adequate information to resolve their own location without revealing anything to the network or others. The message timing required for this method [Fig. 3(d)] can be implemented using a poll-response-final paradigm where one anchor node is the initiator and the other anchor nodes respond. It can also be implemented by having each anchor transmit at a fixed repeating interval. The former method has the advantage of avoiding collisions and was used in our validation experiment, but the latter method has the advantage of homogeneous anchor nodes without a single failure point. The timing and order of anchor transmissions are not important, and a new localization estimation can be computed any time all anchors have transmitted once and one anchor has transmitted twice. If anchor transmissions are happening on a periodic basis, then a location estimate can be made with every anchor transmission, as all TDOAs involving that anchor could be computed, although this may lead to error correlation between consecutive estimates.

1) Derivation: We now derive the equation for $T_\Delta := T_{bs} - T_{as}$ using the information provided by the ranging process in Fig. 3(d). Following loops on the graph produce the following two equations:

$$\begin{aligned} D_{ba} &= S_{ab} - T_{ab} - T_{bs} + T_{as} \\ &= S_{ab} - T_{ab} - T_\Delta \end{aligned} \tag{11}$$

$$\begin{aligned} S_{ba} &= R_{ba} - T_{ab} - T_{bs} + T_{as} \\ &= R_{ba} - T_{ab} - T_\Delta. \end{aligned} \tag{12}$$

Multiplying those together, we get

$$\begin{aligned} S_{ba}D_{ba} = R_{ba}S_{ab} - T_{ab}R_{ba} - T_{ab}S_{ab} + T_{ab}^2 \\ - T_\Delta(S_{ab} + R_{ba} - 2T_{ab} - T_\Delta). \end{aligned} \tag{13}$$

If we reuse (11) to eliminate T_Δ inside the parenthesis and solve for the remaining T_Δ, we arrive at our self-localization TDOA equation

$$T_\Delta = \frac{R_{ba}S_{ab} - S_{ba}D_{ba} - T_{ab}R_{ba} - T_{ab}S_{ab} + T_{ab}^2}{R_{ba} + D_{ba} - T_{ab}}. \tag{14}$$

S_{ba} and S_{ab} are measured directly on the mobile node S while R_{ba} and D_{ab} are measured by anchor B. T_{ab} can be determined from anchor locations or computed in real time using AltDS-TWR [29]. Several equivalent alternative formulations exist by choosing different loops or substitutions. While (14) only contains measurements from anchor B, an alternate formulation can be selected which utilizes measurements from anchor A or from both B and A.

2) Error Bounds: As we did for the source localization equation in Section III-A2, we will now compute the error introduced by using imprecise clocks to measure the time periods required in (5). For time periods that nodes measure directly, we use the error model $\hat{T} = k_i T = (1 + e_i)T$. For TOF between anchor nodes we use the error model $\hat{T}_{ij} = k_i T_{ij}$

or $\hat{T}_{ij} = k_j T_{ij}$ depending on convenience. Using these error models, we can find the worst case error due to clock drift as

$$\begin{aligned}\text{error} &= \hat{T}_\Delta - T_\Delta \\ &= \frac{k_s R_{ba} S_{ab} - k_s S_{ba} D_{ba} - k_a T_{ab} R_{ba} - k_s T_{ab} S_{ab} + k_a T_{ab}^2}{R_{ba} + D_{ba} - T_{ab}} - T_\Delta \\ &\quad e_a \frac{T_{ab}^2 - T_{ab} R_{ba}}{R_{ba} + D_{ba} - T_{ab}} + e_s \frac{R_{ba} S_{ab} - S_{ba} D_{ba} - T_{ab} S_{ab}}{R_{ba} + D_{ba} - T_{ab}}. \end{aligned} \tag{15}$$

The magnitude of worst case error will be less than or equal to that of maximizing the magnitude of each of these terms individually. The left-hand side term can be written as

$$e_a T_{ab} \frac{T_{ab} - R_{ba}}{R_{ba} + D_{ba} - T_{ab}}. \tag{16}$$

The time periods R_{ba} and D_{ba} will both be on the order of tens of milliseconds while T_{ab} will be tens of nanoseconds for an indoor application. We can utilize this to get a rough order-of-magnitude estimate for this term as

$$\frac{1}{2} e_a T_{ab}. \tag{17}$$

For the right-hand side term of (15), we can substitute the equality

$$\begin{aligned} R_{ba} S_{ab} - S_{ba} D_{ba} = T_{ab} R_{ba} + T_{ab} S_{ab} - T_{ab}^2 + T_\Delta R_{ba} \\ + T_\Delta D_{ba} - T_\Delta T_{ab} \end{aligned} \tag{18}$$

to rewrite it as

$$\frac{T_{ab} R_{ba} + T_\Delta R_{ba} + T_\Delta D_{ba} - T_{ab}^2 - T_\Delta T_{ab}}{R_{ab} + D_{ba} - T_{ab}}. \tag{19}$$

This term will achieve the worst case error magnitude when $T_\Delta = T_{ab}$ since $T_{ab} > 0$ and $|T_\Delta| \leq T_{ab}$. We can use the observation that R_{ba} and D_{ba} are the same order of magnitude while T_{ab} is much smaller to get a rough estimate of worst case error for this term as

$$\frac{3}{2} e_s T_{ab}. \tag{20}$$

These two terms are combined to get

$$\text{error} \approx \frac{1}{2} e_a T_{ab} + \frac{3}{2} e_s T_{ab}. \tag{21}$$

Finally, we use the observation that the localizing node generally has a lower quality clock than anchor nodes ($e_a \leq e_s$) to simplify this as

$$\text{error} \approx 2 e_s T_{ab}. \tag{22}$$

3) Comparison to Existing Methods: UWB self-localization methods can be categorized as synchronous or asynchronous depending on whether anchor transmissions happen concurrently or independently. Synchronous methods, such as [43] and [46] require anchor nodes to transmit beacons quasi-simultaneously as shown in Fig. 4(b). Since these beacons arrive at the localizing node with very short relative delays, the transmissions will collide. The localizing node must analyze the CIR to extract TDOA estimates. Since the beacons arrive quasi-simultaneously, clock drift on the localizing node is not a significant factor. However, such methods require very strict anchor synchronization and very high precision control over transmission time. Both [43], [46] recommend a wired anchor backbone to overcome these challenges, but this requirement was primarily to compensate for a shortcoming in the UWB chipset used. Our proposed method differs from synchronous methods in that anchors do not transmit concurrently and synchronization of the anchor network is not required.

Asynchronous methods for UWB self-localization, such as [42], [47], and [48] do not depend on concurrent transmissions from the anchor nodes [Fig. 4(c)] and rely on cooperation between anchors to achieve a reference time or account for clock errors. If each anchor observes the transmission timings of the other anchors, the relative clock errors can be estimated. Our proposed self-localization method depends on this same information but uses a novel equation to utilize it. Most methods, such as [42] and [48] maintain a filtered state of second or third order clock dynamics. This information can be used to correct the naive timing measurements. In contrast, our proposed equation (14) is able to immediately estimate TDOA measurements without the need to maintain any kind of system state. VULoc [47] operates in a similar manner as our proposed method including the same message passing schedule. While both methods can provide similar low error source-localization, VULoc takes a less direct approach than this study through the computation of intermediate "virtual responses." VULoc is also not applicable to source-localization applications.

IV. Experiments

A. Simulation Experiment

In Sections III-A and III-B, we presented our proposed localization methods and derived error bounds. To provide a more complete picture of the proposed methods' performance, we now perform a Monte Carlo simulation [49] of a full localization scenario. While we previously derived worst case performance, the Monte Carlo method provides a complete empirical probability distribution of localization error due to clock drift under a set of assumptions. The following assumptions were used.

1) Eight anchor nodes are positioned as shown in Fig. 5.
2) One mobile node is positioned at a random location within the 128-m^3 capture volume.
3) Each anchor and mobile node has an imperfect clock of similar quality modeled as $\hat{t}_i = (1 + e_i)t + c_i$ where t is the actual time and $\hat{t}_i$ is the observed time by node i. e_i and c_i are both uniform random variables represented as $e_i \sim U(-2 * 10^{-5}, 2 * 10^{-5})$ [28] and $c_i \sim U(0, 100)$ s.
4) The actual time between consecutive transmissions ($R_{b1} - T_{bs}$ and $R_{ab} - T_{ab}$ in Fig. 3(c) and (d), respectively,) is a uniform random variable $X \sim U(0, 0.05)$ s.
5) All other potential sources of error including but not limited to NLOS, hardware variations, calibration error, temperature fluctuations, and antenna orientation are ignored.

The number of Monte Carlo iterations was chosen to ensure convergence of statistical measurements. In our case, one-hundred thousand iterations was adequate.

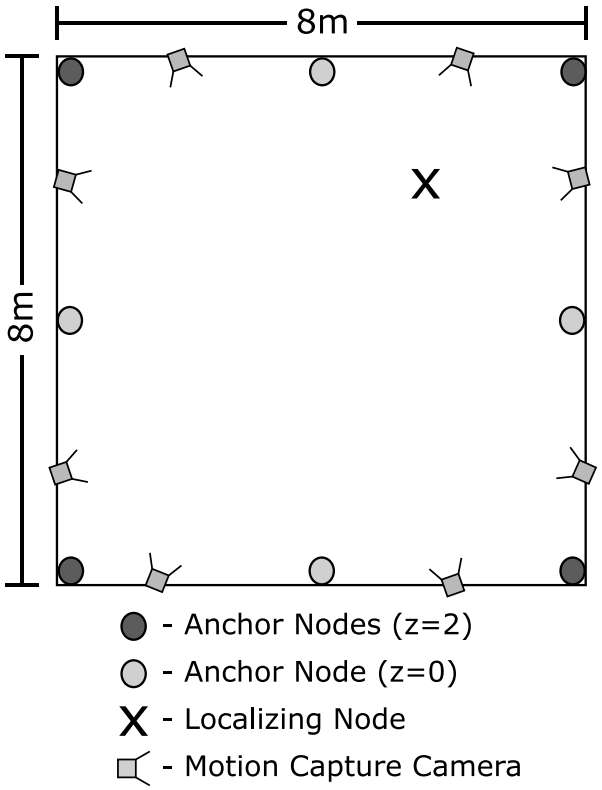

Fig. 5. Experimental setup used for simulation and validation experiments. "z" is the height of each anchor above the capture area shown in meters.

B. NLOS Experiment

The previous simulation experiment assumed ideal environmental conditions and explored the error contribution of clock drift to localization accuracy. This error source was selected as it has been cited in literature as the dominant source of error in many applications [19], [20]. However, challenging environmental conditions, such as NLOS conditions, can also contribute significantly to localization error [50], [51]. In this section we use the Monte Carlo simulation method to explore the effect of NLOS on our proposed localization methods and compare the effect to that on traditional methods. While it is expected that these conditions will decrease localization accuracy, our goal is to compare those effects to those of current methods.

With this aim, we repeat the simulation of eight anchor nodes and one localizing node randomly located within the capture volume (Fig. 5). In contrast to the previous simulation experiment, clock drift is assumed to be zero. Various quantity of human bodies (one, three, and five) are simulated within the capture volume to occlude transmissions. Human bodies have a large effect on signal transmissions due to high water content, the effects of which are characterized in [50]. We use their results to simulate human chest NLOS as a lognormal delay applied to the UWB transmissions ($\mu = 2.78$, $\sigma = 0.18$).

C. Validation Experiment

To validate the performance of our two localization methods, we implemented them in a physical UWB network. The network consisted of nine custom UWB transceivers which used the IEEE 802.15.4a compliant DWM1000 Decawave UWB module (Fig. 6). An onboard STM32 MCU contained our application code, and a micro USB port was used to power and stream ranging results. All anchor nodes and the localizing node used identical hardware and were battery powered without any wired backbone. One anchor node was connected to a lab computer to backhaul results. The eight anchor nodes were arranged around the perimeter of a 64-m^2 capture area as shown in Fig. 5. Anchor nodes in the corners were raised two meters higher than those on the sides of the capture area. All nodes were powered on and allowed to warm up for 10 min to reduce warm-up error. In a real application, this warm-up error can be accounted for, eliminating the need for a warm-up period [52]. The localizing node was then placed at a known location within the capture volume to provide calibration data. Each UWB transceiver has a different antenna delay due to hardware variance which must be accounted for if maximum accuracy is desired. In this study, we followed the procedure presented in [53].

Next, ten trials were performed with the localizing node at different random locations within the capture volume. The UWB network simultaneously performed hyperbolic source-localization, hyperbolic self-localization, and AltDS-TWR localization. This was possible through the usage of Round Robin Ranging as demonstrated for two anchor nodes and one localizing node in Fig. 3(a). All anchor nodes (A and B) and the localizing node (S) broadcast to all other nodes of the network in turn. The Round Robin Ranging method shown in Fig. 3(a) was expanded to include all eight anchor nodes in the validation experiment for a total of nine nodes. The ranging process was repeated for the duration of the trial with the last transmission of one cycle marking the beginning of the next cycle. In other words, each of the nine nodes, including the localizing node, transmitted in turn at an individual rate of 50 Hz or a combined rate of 450 Hz. Since the designation of A and B nodes is arbitrary in Fig. 3, each message transmission can be treated as the conclusion of one Round Robin Ranging cycle which started when that node previously transmitted. That node can thus use the three ranging methods to compute ToF and TDOA with respect to all other nodes in the network. With the completion of each Round Robin Ranging cycle, enough new measurements have been made to perform a complete localization estimate not once, but twice for each of the localization methods. This is because estimates can be made in both directions. For example, Fig. 3(b) shows a range estimate from node A to node S by having A transmit, then S, and finally A again. However, if we wait and consider node S to be the initiating node, we can measure the same range the other direction by considering the transmissions S, A and finally S again when they cycle wraps around. This allows all three localization methods to update in parallel and in real time at a frequency of 100 Hz. While this technique doubles sampling rate (twice the transmission rate of each individual node) and decreases latency, it has the downside that the same period measurements are reused in two consecutive localization estimates leading to possible error correlation issues. This is the case for all three implemented localization methods.

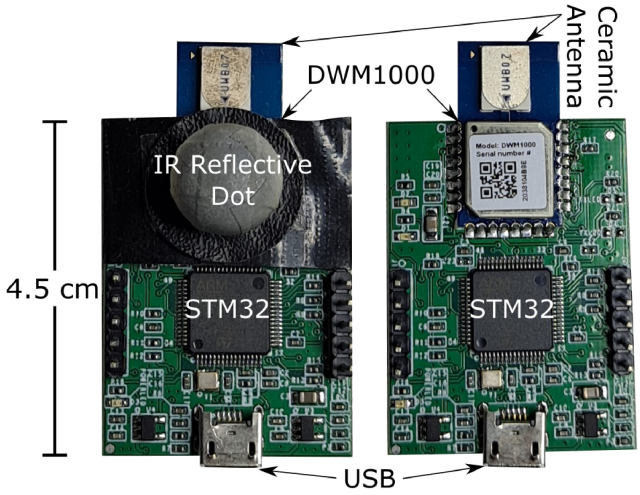

Fig. 6. Custom UWB circuit board with and without reflective IR dot for Vicon visual motion capture. The USB is used to power the node and stream real-time data. Anchor nodes and the localizing node used identical hardware and firmware. All ranging data was wirelessly backhauled to one anchor node which streamed the results to the lab computer for analysis.

TABLE I
SETTINGS FOR THE DW1000 CHIPSET

DW1000 Settings	
Center frequency	3993.6 MHz
Bandwidth	499.2 MHz
PRF	16 MHz
Data rate	110Kbits/s
Preamble length	1024 symbols

Round Robin Ranging was selected as it is a superset of AltDS-TWR, source-localization and self-localization, allowing us to compare all three methods under nearly identical conditions. The necessary time periods were measured on each respective node and then broadcast to the network as the data payload of their ranging message. This gave all nodes in the network the necessary information to perform any or all of the proposed localization methods.

Each node was also equipped with an IR reflective dot which allowed it to be tracked by Vicon optical motion capture cameras which surrounded the capture volume. This provided the reference for our localization methods. The reflective dot is placed directly below the UWB antenna as shown in Fig. 6. This introduces a 2-cm difference between Vicon's reference point and the UWB reference point at the antenna but this error is partially compensated for through calibration. Each of the ten trials was 60-s long and resulted in 6000 location measurements by each of the three localization methods per trial. The settings of the DW1000 chipset are shown in Table I.

V. RESULTS AND DISCUSSION

A. Simulation Experiment

The results of the simulation experiment are shown in Fig. 7. All errors stayed within the theoretical bounds of (8) and (22) for source-localization and self-localization, respectively. The average error was generally an order of magnitude lower than these bounds. Localization in the z-direction was worse than the x and y directions. This was expected as the relatively low diversity of the anchors in that dimension causes a GDOP. A study of optimal anchor placement can be found in [54]. All simulated errors due to clock drift were in the micrometer range. This is well below expected error levels from other sources, such as calibration error, nonisotropic antennas [55], temperature, NLOS [51], and movement [44]. Because of this, these simulation results suggest that the proposed methods effectively eliminate clock drift as an observable source of error and other phenomenon will become dominant.

B. NLOS Experiment

The results of the NLOS experiment are shown in Fig. 8. The localization error is clearly multimodal which can be explained by various NLOS conditions (LOS, 1 body occlusion, 2 body occlusion, etc.). Since eight anchors were used, the effect of outlier errors were likely diminished by the redundant ranging information. Surprisingly, the two proposed methods of hyperbolic source-localization and hyperbolic self-localization performed better under these simulation conditions than the existing methods of AltDS-TWR and traditional TDOA. The slightly worse performance of the traditional TDOA method might be due to the fact that it depends on a single transmission to estimate TDOA compared with three transmissions that the other methods utilize. While magnitudes vary somewhat, the four localization methods appear to be affected by NLOS in a similar fashion.

C. Validation Experiment

The mean magnitudes of localization errors for AltDS-TWR, source-localization, and self-localization in two dimensions were 6.1, 6.9, and 7.5 cm, respectively. In three dimensions localization errors were 11.6, 11.1, and 11.2 cm, respectively. The distributions of location errors in each dimension along with raw ranging error are shown in Fig. 9. The traditional method and two proposed methods all achieved similar localization accuracy which was comparable to the highest accuracy performances from literature [40]. The validation experiment experienced multimodal error which is likely not due to clock drift since it did not appear in the simulation. The error modes appeared correlated with the trials which were each done in a different location. It is possible that this is due to nonisotropic antenna patterns [55] or some other nonlinearity between range and TOF. A small portion of the bias could also be attributed to the separation between the UWB antenna and the Vicon reflective dot. The raw TDOA estimates from the proposed methods experienced more variance than the raw TOF estimates from AltDS-TWR. An increase in variance by up to a factor of two would be expected since TDOA is essentially a difference of two TOFs, involving three nodes instead of two and two wireless channels instead of one.

Our validation experiments involved one localizing node, eight anchor nodes, and 100-Hz location updates. The number of nodes and update frequency could be increased without affecting localization accuracy according to our error derivations (8) and (22). However, if the period of one Round Robin

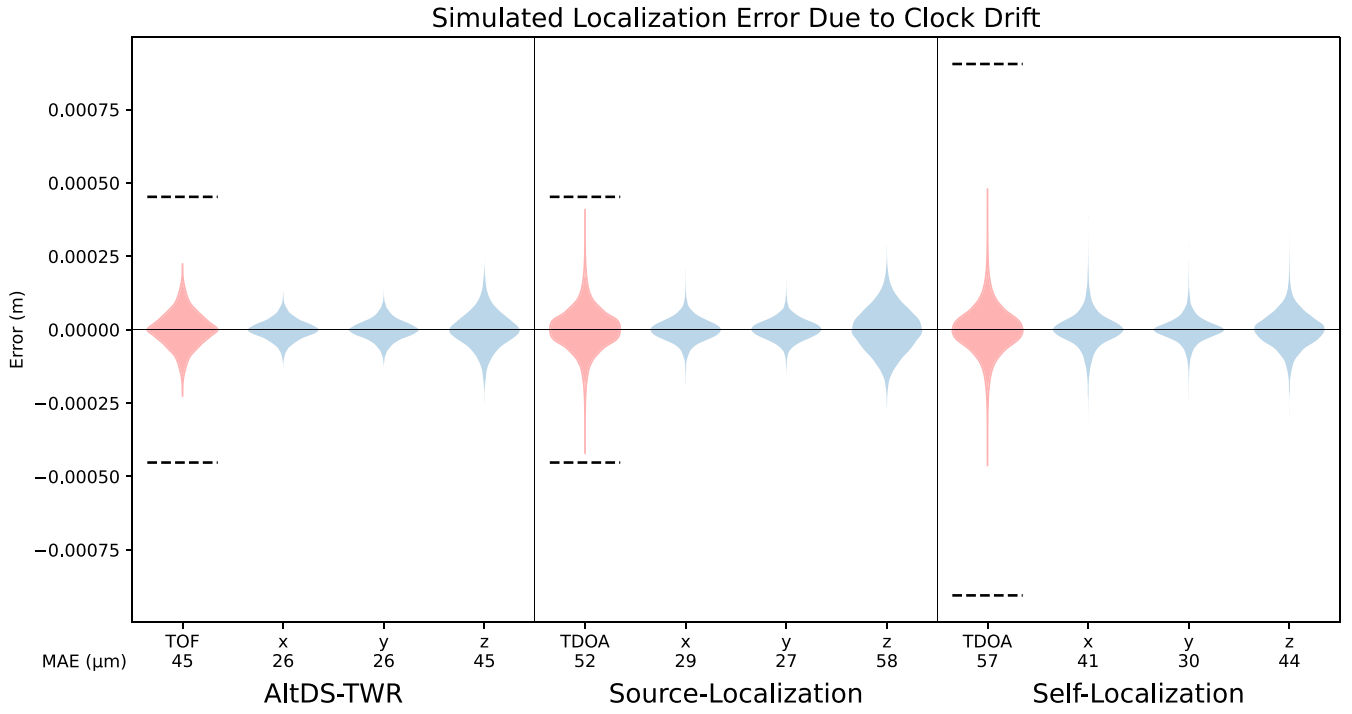

Fig. 7. Simulated localization error due to clock drift from TWR and our two proposed methods. Note that this is error due to a single source and would not reflect the error experienced in real application as other sources would become dominant. This is a Monte Carlo simulation of an indoor localization scenario with 100 000 iterations. The dotted lines are the theoretical worst case errors ([29], (8), and (22), respectively). The mean absolute error (MAE) is shown below each plot in micrometers.

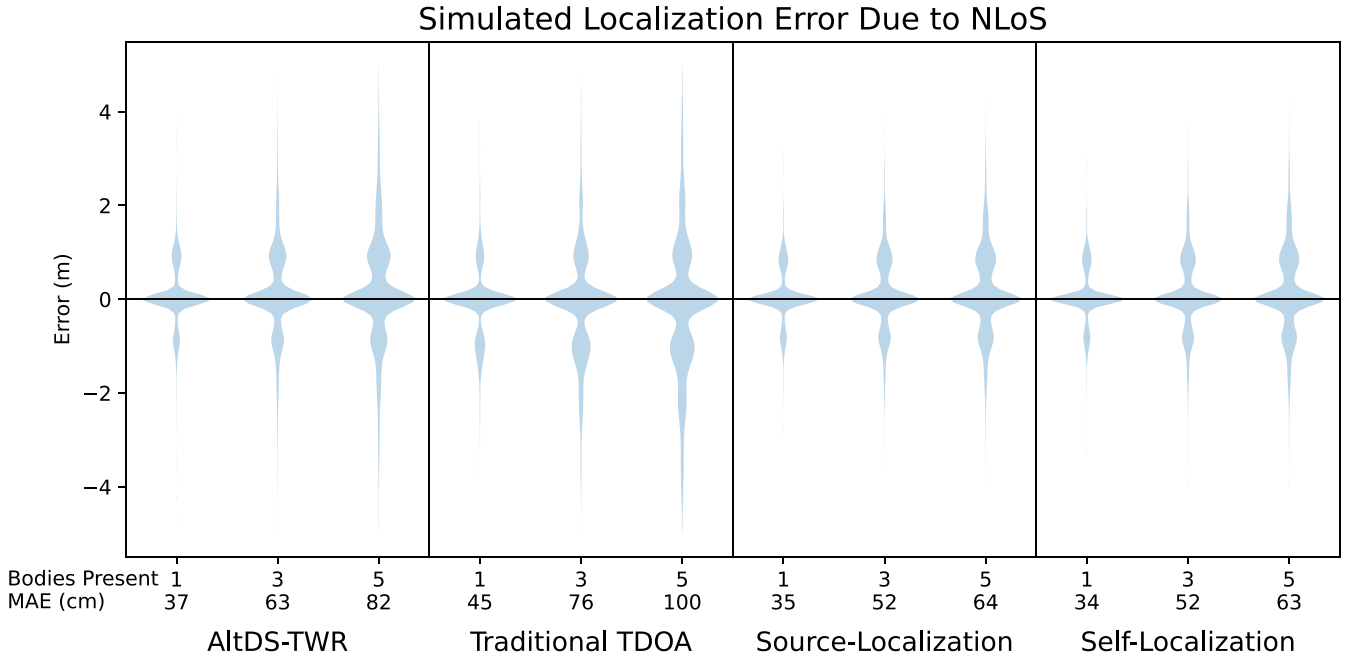

Fig. 8. Simulated localization error due to human body NLOS. One, three, and five human bodies are simulated within the capture area for the two traditional methods on the left and the two proposed methods on the right. As the simulated bodies are in a random location for each of the 100 000 Monte Carlo simulations, NLOS conditions are not present for every iteration. Only error in the x direction is shown in this plot, but the relationship is representative of other dimensions.

Ranging cycle increased significantly, eventually our error model assumption of constant drift would fail, especially if the nodes were exposed to temperature fluctuations [33]. The total rate of transmissions is limited by the need to avoid collisions which, based on data sheets and other works, will be on the order of thousands of hertz [35], [43]. The proposed self-localization method has no limit on the number of tags that can be utilized.

The proposed equations for computing $T\Delta$ [(14) and (5)] have a higher computational cost than traditional TDOA (9)

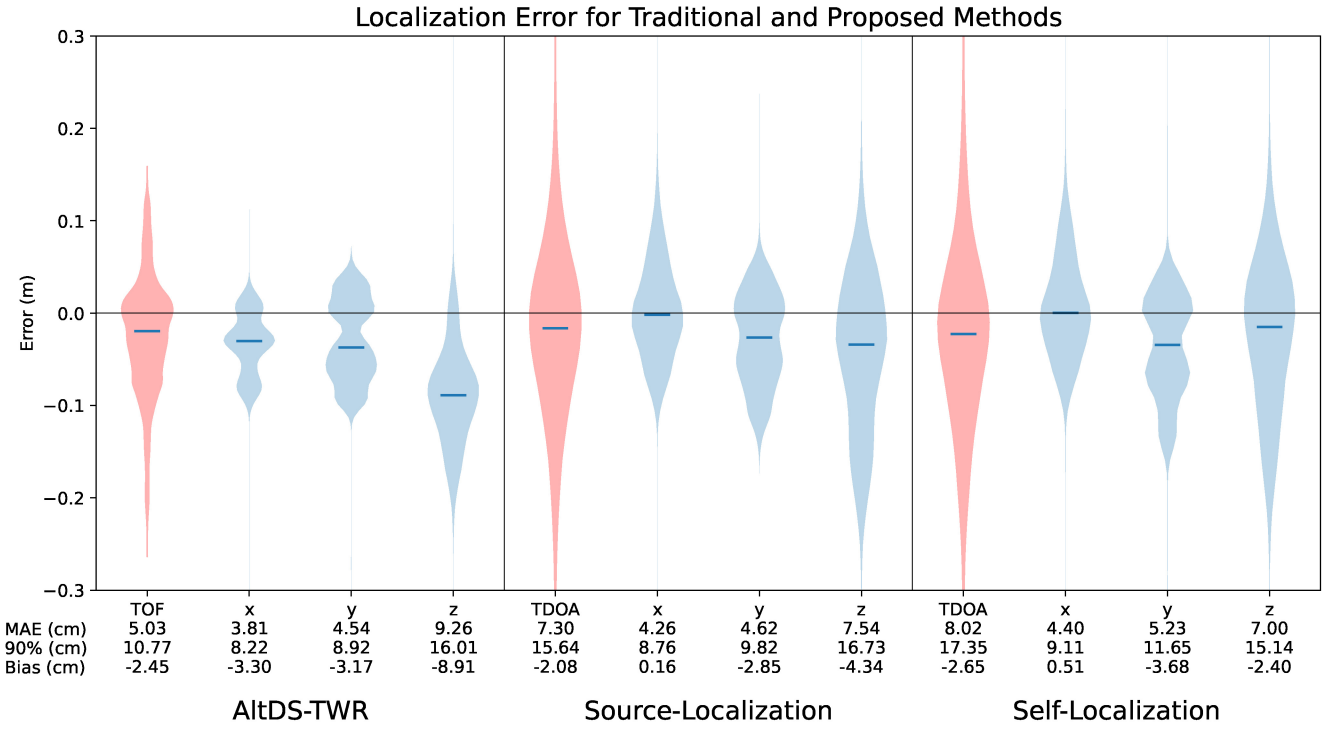

Fig. 9. Combined ranging and localization errors from all validation trials. The MAE, 90th percentile absolute error, and bias are shown below each distribution.

or TOA approaches [29]. However, traditional TDOA needs to additionally implement some synchronization process which likely balances out the comparison. Furthermore, the computation cost of estimating TDOA is negligible compared with the complexity of solving the nonlinear system of equations necessary to resolve location. This process is the same for all methods.

D. Source-Localization

The presented hyperbolic source-localization method is proposed as an alternative to traditional TDOA for tracking applications. The qualitative advantages which our method has over traditional TDOA are summarized in Fig. 1. Crucially, our proposal eliminates the necessity for clock synchronization which could be a limiting factor on performance previously. By doing this, our proposed method offers advantages in the dimensions of accuracy, infrastructure costs, and deployment complexity. Accuracy is improved as it is not dependent on clock synchronization precision. Our proposed method matched the accuracy of best known TOF localization methods (Fig. 9). Anchors can have lower-cost clocks and require no synchronization process, which can dramatically decrease their size and complexity, even making them wireless as in this study. Deployment complexity is dramatically reduced as knowing the exact location of all anchor nodes is not necessary. Anchor nodes can determine their relative positioning with high accuracy in real time. An anchor being bumped or moved will not affect the accuracy of localization.

Our proposed hyperbolic source-localization method maintains many of the strengths of traditional TDOA methods. No change to tag design or behavior is required by our method, and tags can maintain a small size and long battery lives as no signal reception or signal processing is required.

The disadvantages of our proposed method compared with the traditional TDOA is that anchor nodes must make transmissions and listen to transmissions from each other. The maximum number of tags is decreased in proportion to the number of anchors due to the requirement for anchors to transmit messages. This is not a significant detriment in some situations as the number of tags is much greater than the number of anchors in many tracking applications. The latency of localization is also increased by up to the period of the ranging process.

Compared with TOF-based approaches, our proposed hyperbolic source-localization method can provide the same accuracy without requiring the mobile node to do any listening or range computation resulting in dramatic decrease of power usage, decreased mobile node complexity, and increased node counts. Using existing TDOA system tags as an indicator, this improvement can be several orders of magnitude.

While error due to clock drift was effectively eliminated as an error source in the scenarios we explored, this error does increase with distance and could become significant at large distances. Based on the error behavior derived in (8), clock drift would reemerge as a significant source of error if localization distances exceed 10's of kilometers while using the same low-cost clocks considered in this study.

E. Self-Localization

The presented hyperbolic self-localization method is proposed as an alternative to TOF and TWR methods, namely, AltDS-TWR in navigation applications. The qualitative

advantages which our method has over AltDS-TWR are summarized in Fig. 1. The core advantage of our method is that the localizing node is not required to make any transmissions. Because of this, infinite localizing node density and high privacy can be achieved. Our proposed method matches the localization accuracy achieved by AltDS-TWR (Fig. 9). The disadvantage of our method compared with AltDS-TWR is that only the localizing node is aware of location information, hyperbolic self-localization cannot be used for tracking applications. AltDS-TWR on the other hand has the flexibility to be used in either tracking or navigation applications.

Compared with the proposed hyperbolic source-localization, hyperbolic self-localization experiences clock drift error inversely proportional to the quality of the mobile node as opposed to only quality of the anchor nodes. This is notable since many applications can afford to place more accurate clocks on anchor nodes than on mobile nodes. This is because anchor nodes are stationary and are often few in number compared with mobile nodes. Based on error limits derived in (22), clock drift error will not be a significant source of localization error unless distances reach 10's of kilometers or more.

VI. Conclusion

In this work, we proposed two new hyperbolic localization methods which are well suited for indoor UWB tracking and navigation. We demonstrated that localization accuracy achieved by both methods is unsurpassed by current alternatives. Furthermore, our methods provide significant application benefits. Our source-localization method for tracking applications can achieve greater accuracy with lower infrastructure requirements and lower-cost nodes. Our self-localization method for navigation applications can provide infinite localization node density and high security.

References

[1] R. L. Frank, "Current developments in Loran-C," *Proc. IEEE*, vol. 71, no. 10, pp. 1127–1139, Oct. 1983.

[2] S. Vatansever and I. Butun, "A broad overview of GPS fundamentals: Now and future," in *Proc. IEEE 7th Annu. Comput. Commun. Workshop Conf. (CCWC)*, 2017, pp. 1–6.

[3] R. Li et al., "Advances in BeiDou navigation satellite system (BDS) and satellite navigation augmentation technologies," *Satell. Navigat.*, vol. 1, no. 1, pp. 1–23, 2020. [Online]. Available: https://doi.org/10.1186/s43020--020-00010--2

[4] J. P. Bartolomé, X. Maufroid, I. F. Hernández, J. A. López Salcedo, and G. S. Granados, *Overview of Galileo System*. Dordrecht, The Netherlands: Springer, 2015, pp. 9–33.

[5] J. A. Del Peral-Rosado, R. Raulefs, J. A. López-Salcedo, and G. Seco-Granados, "Survey of cellular mobile radio localization methods: From 1G to 5G," *IEEE Commun. Surveys Tuts.*, vol. 20, no. 2, pp. 1124–1148, 2nd Quart., 2018.

[6] F. Zafari, A. Gkelias, and K. K. Leung, "A survey of indoor localization systems and technologies," *IEEE Commun. Surveys Tuts.*, vol. 21, no. 3, pp. 2568–2599, 3rd Quart., 2019.

[7] P. Dabove, V. Di Pietra, M. Piras, A. A. Jabbar, and S. A. Kazim, "Indoor positioning using ultra-wide band (UWB) technologies: Positioning accuracies and sensors' performances," in *Proc. IEEE/ION Position Location Navigat. Symp. (PLANS)*, 2018, pp. 175–184.

[8] T. K. Geok et al., "Review of indoor positioning: Radio wave technology," *Appl. Sci.*, vol. 11, no. 1, pp. 1–44, 2021.

[9] L. Flueratoru, S. Wehrli, M. Magno, E. S. Lohan, and D. Niculescu, "High-accuracy ranging and localization with ultrawideband communications for energy-constrained devices," *IEEE Internet Things J.*, vol. 9, no. 10, pp. 7463–7480, May 2022.

[10] M. Kok, J. D. Hol, and T. B. Schön, "Indoor positioning using ultrawideband and inertial measurements," *IEEE Trans. Veh. Technol.*, vol. 64, no. 4, pp. 1293–1303, Apr. 2015.

[11] M. Singh, M. Roeschlin, E. Zalzala, P. Leu, and S. Čapkun, "Security analysis of IEEE 802.15.4z/HRP UWB time-of-flight distance measurement," in *Proc. ACM Conf. Secur. Privacy Wireless Mobile Netw.*, 2021, pp. 227–237.

[12] G. Heidari, *WiMedia UWB: Technology of Choice for Wireless USB and Bluetooth*. New York, NY, USA: Wiley, 2008.

[13] R. J. Fontana and S. J. Gunderson, "Ultra-wideband precision asset location system," in *IEEE Conf. Ultra Wideband Syst. Technol. Dig. Papers (UWBST)*, 2002, pp. 147–150.

[14] L. Eadicicco, "Apple and samsung newest phones use a little-known technology that lets your phone understand exactly where it is—And could mean you never misplace anything again," Bus. Insider, New York, NY, USA, Aug. 2020. [Online]. Available: https://www.businessinsider.com/uwb-explained-samsung-galaxy-note-ultra-apple-iphone-features-airdrop-2020--8

[15] S. Gollister, "Samsung partners with Audi, BMW, ford, and genesis to turn your phone into a car key." Verge, Washington, DC, USA, Jan. 2021. [Online]. Available: https://www.theverge.com/2021/1/14/22230960/samsung-digital-car-key-audi-bmw-ford-genesis-uwb-bluetooth

[16] K. Wen, K. Yu, and Y. Li, "NLOS identification and compensation for UWB ranging based on obstruction classification," in *Proc. 25th Eur. Signal Process. Conf. (EUSIPCO)*, 2017, pp. 2704–2708.

[17] A. Alarifi et al., "Ultra wideband indoor positioning technologies: Analysis and recent advances," *Sensors*, vol. 16, no. 5, pp. 1–36, 2016.

[18] J. J. Pérez-Solano, S. Ezpeleta, and J. M. Claver, "Indoor localization using time difference of arrival with UWB signals and unsynchronized devices," *Ad Hoc Netw.*, vol. 99, Mar. 2020, Art. no. 102067. [Online]. Available: https://doi.org/10.1016/j.adhoc.2019.102067

[19] T. Wang, X. Chen, N. Ge, and Y. Pei, "Error analysis and experimental study on indoor UWB TDoA localization with reference tag," in *Proc. 19th Asia-Pac. Conf. Commun. (APCC)*, 2013, pp. 505–508.

[20] X. Li, Z. D. Deng, L. T. Rauchenstein, and T. J. Carlson, "Contributed review: Source-localization algorithms and applications using time of arrival and time difference of arrival measurements," *Rev. Sci. Instrum.*, vol. 87, no. 4, 2016, Art. no. 41502. doi: 10.1063/1.4947001.

[21] M. Laaraiedh, L. Yu, S. Avrillon, and B. Uguen, "Comparison of hybrid localization schemes using RSSI, TOA, and TDOA," in *Proc. 17th Eur. Wireless Sustain. Wireless Technol.*, 2011, pp. 1–5.

[22] S. Uluskan and T. Filik, "A survey on the fundamentals of RSS based localization," in *Proc. SIU*, 2016, pp. 1633–1636.

[23] R. Faragher and R. Harle, "Location fingerprinting with bluetooth low energy beacons," *IEEE J. Sel. Areas Commun.*, vol. 33, no. 11, pp. 2418–2428, Nov. 2015.

[24] H. Li and Z. Cheng, "Angle-of-arrival estimation using difference beams in localized hybrid arrays," *Sensors*, vol. 21, no. 5, pp. 1–11, 2021.

[25] I. Dotlic, A. Connell, H. Ma, J. Clancy, and M. McLaughlin, "Angle of arrival estimation using decawave DW1000 integrated circuits," in *Proc. 14th Workshop Position. Navigat. Commun. (WPNC)*, 2018, pp. 1–6.

[26] X. Zhu, T. Qiu, W. Qu, X. Zhou, M. Atiquzzaman, and D. Wu, "BLS-location: A wireless fingerprint localization algorithm based on broad learning," *IEEE Trans. Mobile Comput.*, vol. 22, no. 1, pp. 115–128, Jan. 2023.

[27] X. Zhu, W. Qu, T. Qiu, L. Zhao, M. Atiquzzaman, and D. O. Wu, "Indoor intelligent fingerprint-based Localization: Principles, approaches and challenges," *IEEE Commun. Surveys Tuts.*, vol. 22, no. 4, pp. 2634–2657, 4th Quart., 2020.

[28] *IEEE Standard for Information Technology-Telecommunications and Information Exchange Between Systems-LANs and MANs-Specific Requirements-Part 15.4: Wireless MAC and PHY Specifications for LR-WPANs-Amendment 1: Add Alternate PHYs*, IEEE Standard 802.15.4a-2007, Aug. 2007.

[29] D. Neirynck, E. Luk, and M. McLaughlin, "An alternative double-sided two-way ranging method," in *Proc. 13th Workshop Position. Navigat. Commun. (WPNC)*, 2017, pp. 16–19.

[30] D. P. Young, C. M. Keller, D. W. Bliss, and K. W. Forsythe, "Ultra-wideband (UWB) transmitter location using time difference of arrival (TDOA) techniques," in *Proc. Asilomar Conf. Signals Syst. Comput.*, vol. 2, 2003, pp. 1225–1229.

[31] J. Xu, M. Ma, and C. L. Law, "Position estimation using UWB TDOA measurements," in *Proc. IEEE Int. Conf. Ultra Wideband (ICUWB)*, 2006, pp. 605–610.

[32] R. Mazraani, M. Saez, L. Govoni, and D. Knobloch, "Experimental results of a combined TDOA/TOF technique for UWB based localization systems," in *Proc. IEEE Int. Conf. Commun. Workshops (ICC)*, 2017, pp. 1043–1048.
[33] D. Vecchia, P. Corbalan, T. Istomin, and G. P. Picco, "TALLA: Large-scale TDoA localization with ultra-wideband radios," in *Proc. Int. Conf. Position. Indoor Navigat. (IPIN)*, 2019, pp. 1–8.
[34] W. Wang, J. Huang, S. Cai, and J. Yang, "Design and implementation of synchronization-free TDOA localization system based on UWB," *Radioengineering*, vol. 28, no. 1, pp. 320–330, 2019.
[35] S. Bottigliero, D. Milanesio, M. Saccani, and R. Maggiora, "A low-cost indoor real-time locating system based on TDOA estimation of UWB pulse sequences," *IEEE Trans. Instrum. Meas.*, vol. 70, 2021, Art. no. 5502211.
[36] "Getting back to basics with ultra-wideband (UWB)," Qorvo, Greensboro, NC, USA, Rep. 202105, May 2021.
[37] G. Shi and Y. Ming, "Survey of indoor positioning systems based on ultra-wideband (UWB) technology," in *Lecture Notes in Electrical Engineering*, vol. 348. New Delhi, India: Springer, 2016, pp. 1269–1278.
[38] "Application note: APS007 wired synchronization of anchor nodes in a TDOA real time location," Decawave, Qorvo, Greensboro, NC, USA, Rep. APS007, 2014.
[39] Y. Xue, W. Su, H. Wang, D. Yang, and J. Ma, "A model on indoor localization system based on the time difference without synchronization," *IEEE Access*, vol. 6, pp. 34179–34189, 2018.
[40] S. He and X. Dong, "High-accuracy localization platform using asynchronous time difference of arrival technology," *IEEE Trans. Instrum. Meas.*, vol. 66, no. 7, pp. 1728–1742, Jul. 2017.
[41] J. Zhou, L. Shen, and Z. Sun, "A new method of D-TDOA time measurement based on RTT," in *Proc. MATEC Web Conf.*, vol. 207, 2018, pp. 1–5.
[42] A. Ledergerber, M. Hamer, and R. D'Andrea, "A robot self-localization system using one-way ultra-wideband communication," in *Proc. IEEE Int. Conf. Intell. Robots Syst.*, vol. 2015, 2015, pp. 3131–3137.
[43] B. Großwindhager, M. Stocker, M. Rath, C. A. Boano, and K. Römer, "SnapLoc: An ultra-fast UWB-based indoor localization system for an unlimited number of tags," in *Proc. Inf. Process. Sensor Netw. (IPSN)*, 2019, pp. 61–72.
[44] T. Risset, C. Goursaud, X. Brun, K. Marquet, and F. Meyer, "UWB ranging for rapid movements," in *Proc. 9th Int. Conf. Indoor Position. Indoor Navigat. (IPIN)*, 2018, pp. 1–8.
[45] D. J. Torrieri, "Statistical theory of passive location systems," *IEEE Trans. Aerosp. Electron. Syst.*, vol. AES-20, no. 2, pp. 183–198, Mar. 1984.
[46] P. Corbalán, G. P. Picco, and S. Palipana, "Chorus: UWB concurrent transmissions for GPS-like passive localization of countless targets," in *Proc. Inf. Process. Sensor Netw. (IPSN)*, 2019, pp. 133–144.
[47] J. Yang, B. S. Dong, and J. Wang, "VULoc: Accurate UWB Localization for countless targets without Synchronization," *Proc. ACM Interact. Mobile Wearable Ubiquitous Technol.*, vol. 6, no. 3, pp. 1–25, 2022.
[48] M. Hamer and R. D'Andrea, "Self-calibrating ultra-Wideband network supporting multi-robot localization," *IEEE Access*, vol. 6, pp. 22292–22304, 2018.
[49] S. Raychaudhuri, "Introduction to Monte Carlo simulation," in *Proc. Winter Simulat. Conf.*, 2008, pp. 91–100.
[50] L. Xia, S. Redfield, and P. Chiang, "Experimental characterization of a UWB channel for body area networks," *EURASIP J. Wireless Commun. Netw.*, vol. 2011, Jan. 2011, Art. no. 703239.
[51] J. Khodjaev, Y. Park, and A. Saeed Malik, "Survey of NLOS identification and error mitigation problems in UWB-based positioning algorithms for dense environments," *Ann. Telecommun.*, vol. 65, nos. 5–6, pp. 301–311, 2010.
[52] J. Sidorenko, V. Schatz, N. Scherer-Negenborn, M. Arens, and U. Hugentobler, "DecaWave ultra-wideband warm-up error correction," *IEEE Trans. Aerosp. Electron. Syst.*, vol. 57, no. 1, pp. 751–760, Feb. 2021.
[53] "APS014: DW1000 antenna delay calibration version 1.2," Decawave, Qorvo, Greensboro, NC, USA, Rep. APS014, 2018.
[54] J. T. Isaacs, D. J. Klein, and J. P. Hespanha, "Optimal sensor placement for time difference of arrival Localization," in *Proc. IEEE Conf. Decis. Control*, 2009, pp. 7878–7884.
[55] B. Merkl, A. Fathy, and M. Mahfouz, "Base station orientation calibration in 3-D indoor UWB positioning," in *Proc. IEEE Int. Conf. Ultra Wideband (ICUWB)*, vol. 1, 2008, pp. 93–96.

David Chiasson received the B.S. degree in electrical and computer engineering from Purdue University, West Lafayette, IN, USA, in 2012, and the M.S. degree in electrical engineering from Stanford University, Stanford, CA, USA, in 2014. He is currently pursuing the Ph.D. degree with the State Key Laboratory of Mechanical System and Vibration, School of Mechanical Engineering, Shanghai Jiao Tong University, Shanghai, China.

His research interests include body area networks, signal processing, and wireless communications.

Yuan Lin (Graduate Student Member, IEEE) received the B.E. degree in mechanical engineering from Jilin University, Jilin, China, in 2019. He is currently pursuing the Ph.D. degree in mechanical engineering from the School of Mechanical Engineering, Shanghai Jiao Tong University, Shanghai, China.

His research interests include soft acoustic waveguides for strain and pressure sensing, and their applications in wearable hand gesture recognition and wearable haptics.

Manon Kok received the B.S. degree in applied physics, the first M.S. degree in philosophy of science, technology and society, and the second M.S. degree in applied physics from the University of Twente, Enschede, The Netherlands, in 2005, 2007, and 2009, respectively, and the Ph.D. degree in automatic control from Linköping University, Linköping, Sweden, in 2017.

She was a Research Associate with the University of Cambridge, Cambridge, U.K., from 2017 to 2018. She is currently an Assistant Professor with the Delft Center for Systems and Control, Delft University of Technology, Delft, The Netherlands. Her research interests lie in the fields of probabilistic modeling for sensor fusion, signal processing, and machine learning.

Peter B. Shull (Member, IEEE) received the B.S. degree in mechanical engineering and computer engineering from LeTourneau University, Longview, TX, USA, in 2005, and the M.S. and Ph.D. degrees in mechanical engineering from Stanford University, Stanford, CA, USA, in 2008 and 2012, respectively.

He was a Postdoctoral Fellow with the Bioengineering Department, Stanford University from 2012 to 2013. He is a Professor of Mechanical Engineering with Shanghai Jiao Tong University, Shanghai, China. He has performed pioneering research involving human–computer interaction, hand gesture recognition, wearable systems, and real-time movement sensing and feedback to improve human health and performance in medical and sports applications. He has 18 competitive research grants, authored 86 peer-reviewed journal articles and conference papers, and delivered 55 academic technical presentations in English and Chinese. He has been the Primary Academic Advisor for 26 master's, doctoral, and postdoctoral researchers.

Prof. Shull is an Associate Editor for Nature *npj Digital Medicine*, IEEE JOURNAL OF BIOMEDICAL AND HEALTH INFORMATICS, IEEE TRANSACTIONS ON NEURAL SYSTEMS AND REHABILITATION ENGINEERING, and *Wearable Technologies*.